The Situation of Global Dimming in the Regional Major Cities of Thailand: Shedding Light on a Growing Concern

Mahawan, N.,[1] Charoentrakulpeeti, W.[2*] and Suwanprasit, C.[2]
[1]Faculty of Architecture and Environmental Design, Maejo University, Thailand
E-mail: nikorn512@yahoo.com
[2]Department of Geography, Faculty of Social Sciences, Chiang Mai University, Thailand
E-mail: wanpen.c@cmu.ac.th,* chanida.suwanprasit@gmail.com
**Corresponding Author*

DOI: https://doi.org/10.52939/ijg.v19i9.2883

Abstract
The reduction in surface solar radiation known as "Global Dimming" has significant repercussions for both human and ecological well-being. There is a need for further empirical evidence to better understand the extent of Global Dimming in Southeast Asia, particularly in Thailand. This study aims to examine Surface Solar Radiation (SSR) and Aerosol Optical Thickness (AOT) trends and their relationships before the 1990s and post-1990s using ground station data and satellite images to investigate land use of five provinces: Bangkok, Chiang Mai, Songkla, Rayong, and Kon Khen. AOT does not rise significantly annually, but in the central region during the summer, it increases with a significance level of 0.05, and March is the most significant monthly change. SSRavg trend was unchanged before the 1990s. After the 1990s, SSRavg decreased significantly in the central, northern, and eastern regions, with a significance level of 0.01, especially in winter. AOT correlates positively with surface temperature and negatively with SSR intensity and relative humidity. AOT is positively correlated with built-up cover types and negatively correlated with forest cover types (R^2 values of 0.708). These findings reveal that Thailand is entering a global dimming; hence, managing land cover could lessen air pollution and help future preventative efforts.

Keywords: Aerosol Optical Thickness, Dimming, Land Cover, Surface Solar Radiation, Thailand

1. Introduction

The issue of global climate change holds great significance and has attracted considerable attention as societies endeavor to identify comprehensive measures to alleviate its consequences. The dominant focus of public discourse pertains to the idea of global warming. However, it is important to acknowledge the existence of another climate-related phenomenon, namely global dimming, which has emerged alongside global warming but remains relatively unfamiliar to the public. Global dimming, which refers to the decrease in solar radiation reaching the Earth's surface, has substantial consequences for humanity that are equally serious to those related to global warming. The potential consequences of global dimming on the monsoon winds in Asia are of significant interest, as they play a crucial role in contributing around 50 percent of the world's precipitation. This, in turn, can result in droughts and food scarcity. Stanhill and Moreshet [1] conducted an initial investigation on the phenomena of declining solar radiation intensity throughout the period from 1958 to 1985. The examination of survey data during that specific timeframe unveiled a decrease of 9% in solar radiation intensity inside the Antarctic continental region. Similarly, the Americas, Europe, and Russia observed 10%, 16%, and 30% corresponding reductions. The worldwide solar radiation intensity experienced a decrease of 22%. It is worth noting that global dimming is primarily observed in the northern hemisphere.

Solar radiation intensity variations can arise from both exogenous and endogenous factors [2]. Even though variations in solar output over long durations (10,000–100,000 years) can somewhat affect global dimming, they have little effect over shorter timescales, like decades.

Direct measurements of solar radiation reflectance off Earth have demonstrated a link with the 11-year Sunspot Cycle, demonstrating a negligible impact on the reflected solar radiation. Therefore, when assessing changes in solar radiation intensity incident on the Earth's surface, extraterrestrial causes can be discounted. As a result, the phenomenon of global dimming is primarily caused by changes in elements of the Earth's atmosphere, specifically the characteristics of different aerosols that affect radiation absorption and diffusion. Aerosol compounds like sulfate, black carbon, and particulate matter are present and contribute significantly to both global dimming and warming, accounting for 50% of their combined impact [3]. The amount of aerosols in the atmosphere varies geographically and rises as a result of human activities like industrial production and transportation. Notably, the incident solar radiation intensity dropped by 58 W/m^2 between 1958 and 1985 without any change in cloud cover, showing a strong association with an increase in automobile emissions on surrounding roadways [4]. Furthermore, illustrating the impact of pollution and aerosols on solar radiation intensity reaching the Earth's surface are studies by Alpert and Kishcha [5] that have clearly shown cases of global dimming in densely populated urban regions.

Aerosols also have unintended consequences since they act as water vapor condensation nuclei and cause clouds to form. The status of clouds in the atmosphere is greatly impacted by these aerosol-induced changes in cloud content and appearance intervals. Additionally, heat-absorbing particles that are dispersed in the air prevent the formation of new clouds or cause existing ones to dissipate (the semidirect effect). Overall, increased dimming caused by aerosols in the atmosphere contributes significantly to the reduction of solar radiation. Between 1950 and 1980, a decrease in the strength of solar radiation reaching the Earth's surface drew attention to the study of global dimming. A general consensus has arisen that changes in incident solar radiation intensity can be split into two different periods: the dimming period prior to 1990 and the brightening period after 1990 [2].

Reports of a global dimming phenomenon appeared in several places between 1960 and 1990. Between 1954 and 1995, Ireland suffered a dimming incidence rate of -3.5 W/m^2, with a 2% drop in the relative trend per period [6]. According to Russak [7], Estonia recorded a global dimming rate of -5.2 W/m^2 between 1955 and 1986, with a relative trend decline of -5% per time period. Germany documented a dimming incidence of -6 W/m^2 from 1964 to 1990, with a relative trend decline of -4% per period [8]. Switzerland showed the most considerable reduction in global dimming, with an incidence rate of -10 W/m^2 from 1960 to 1980 and a relative fall of -7% for that time period [9]. In contrast, Turkey had the lowest dimming incidence rate of any country in continental Europe, with a rate of -2 W/m^2 from 1960 to 1994 and a relative trend decline of -1% per period [10]. From 1954 to 1994, Israel witnessed a dimming incidence of -8.8 W/m^2 with a relative trend rate decline of -5% per period [11]. According to Abakumova et al., [12], Moscow, Russia, experienced a dimming incidence of -3.1 W/m^2 between 1958 and 1993 with a relative decline of -2% per period. According to Norris and Wild [13], between 1971 and 1986, Europe saw an overall dimming rate of -3.1 W/m^2 and a relative reduction of -2.3% per period. In Asia, the Soviet Union (-1 to -8 W/m^2 between 1958 and 1992), China (-7 W/m^2 from 1961 to 1989), and India (-2.9 W/m^2 between 1966 and 1990) were among the nations that reported on the global dimming phenomenon before 1960. Notably, countries with constrained space, such as Japan (-1.3 W/m^2 between 1971 and 1989) and the Hong Kong Special Administrative Region (-18 W/m^2 between 1971 and 1989), also experienced global dimming [14] [15] [16] and [17].

However, Southeast Asia, including Thailand, has not seen any reports of the dimming phenomenon. The emergence of interest in the issue of global dimming in Africa can be traced back to the 1960s. According to reports, large desert nations like Namibia and Cairo, Egypt experienced significant global dimming as a result of desert aerosols (-5.4 W/m^2 between 1960 and 1990) and -13 W/m^2 between 1968 and 1994 [18] and [19]. According to Liley [20], between 1954 and 1990, New South Wales in Australia had global dimming at a rate of -4.8 W/m^2. North America also showed global dimming, with rates of -6 W/m^2 in the United States from 1961 to 1990 [21], -2.6 W/m^2 in Canada from 1958 to 1999 [22]. However, South America has not received any reports on the phenomena of global dimming. Like other geographical areas, the polar regions have also been subject to the measurable impacts of the global dimming phenomena. According to the research conducted by Stanhill and Cohen [23], it was seen that there was a negative radiative forcing of -2.8 W/m^2 in the polar regions from 1957 to 1994. Similarly, a negative radiative forcing of -3.8 W/m^2 in the Arctic region was recorded from 1950 to 1993 [24]. After 1990, the world's fading rate changed to brighter.

Since the onset of the global brightening phenomenon in the early 1990s, countries across the globe have undertaken measures to address the issue of global warming. These efforts have been mostly channeled through international agreements such as the United Nations Framework Convention on Climate Change, as well as specific protocols like the Montreal Protocol and the Kyoto Protocol. Incidence of global brightening was 2.2 W/m^2 from 1986 to 2000, according to research by [25] Germany has the highest prevalence of global brightening in Europe between the years 1985 and 2005, at 4.6 W/m^2 [2]. According to a study conducted by Sanchez-Lorenzo et al., [26], Switzerland had an increase in radiative forcing of 2.6 W/m^2 between 1981 and 2005. In the period from 1987 to 2002, Europe observed an increase in radiative forcing of 1.4 W/m^2, as reported by Norris and Wild [13]. In Asia, post-1990 data on the global dimming phenomenon indicated an increase in the brightening rate compared to the period before 1960, suggesting a reduction in atmospheric pollution due to the adoption of cleaner technologies in industrial production. For example, China experienced a brightening rate of 2.7 W/m^2 during the period 1990-2000 [16], while Japan, a country with spatial constraints and high population density, exhibited the highest brightening rate in Asia at 8 W/m^2 during the period 1990-2002. Conversely, India saw an increase in the incidence of global dimming from 1984 to 2001, with a rate of -8.6 W/m^2 [27]. New Zealand experienced a brightening incidence rate of 0.5 W/m^2 between 1990 and 2008 [20]. In North America, global brightening was observed in Oregon, United States, with a rate of 2 W/m^2 to 3 W/m^2 from 1980 to 2007 [28]. The South Pole region exhibited a trend of increasing brightening, with a rate of 4.1 W/m^2 from 1992-2004 [2].

The phenomenon of transitioning from dimming to brightening was seen in locations that had high levels of industry and transportation prior to the 1990s. However, after the 1990s, production centers moved to developing nations, while wealthy countries adopted cleaner technology, which reduced the phenomena of dimming and led to the creation of brightening patterns. However, there is still a dearth of empirical evidence for dimming phenomenon in Asia and Africa, particularly in Thailand. Hence, the primary objective of the research is to enhance comprehension of the phenomenon of global dimming in Thailand. This will be achieved through an examination of alterations in solar radiation intensity reaching the Earth's surface, coupled with an analysis of the interplay between aerosol, climate-related variables (such as solar radiation intensity, temperature, and air humidity), and physical factors (specifically, land cover ratio). This study's findings will contribute to identifying potential strategies for mitigating the phenomenon of global dimming, specifically in Thailand while addressing the broader concern of global warming. As a result, Thailand must comprehend the effects of global dimming fully.

2. Methodology

This study aims to provide empirical evidence regarding the occurrence of global dimming in Thailand. The research methodology involves comprehensive data collection from multiple sources, including statistical data obtained from meteorological stations and spatial data acquired through remote sensing platforms. The statistical data is utilized to analyze Aerosol Optical Thickness (*AOT*) and solar radiation situations, employing regression models to investigate correlations between *AOT* and land cover types, thereby elucidating the dimming phenomenon in Thailand (Figure 1). Studying changes in solar radiation poses challenges due to the limited availability of direct solar radiation measurement data in Thailand. However, alternative approaches are employed to estimate the amount of solar radiation reaching the Earth's surface, namely Diurnal Temperature Range, Sunshine Duration, Pan Evaporation, and Planetary Albedo [2], are incorporated into a developed model. According to the Diurnal Temperature Range, Serm Chanchai [29] implemented a model based on the principle that air temperature and solar radiation are related to the transmission of heat energy in the atmosphere. In order to estimate solar radiation values, air temperature data can be employed. This research applied such model, based on the difference between the daily maximum and minimum air temperature to analyze the trend of solar radiation intensity changes during the pre-1990 (1951-1990) and post-1990 periods. This period division aligns with the global dimming/brightening phenomenon observed worldwide, allowing for comprehensive insights into solar radiation trends in Thailand.

Regarding spatial data on land cover ratios, Landsat 8 satellite images with a spatial resolution of 30 meters obtained from the United States Geological Survey (https://earthexplorer.usgs.gov/) are utilized with 7 images acquired in February 2017 for the areas of Chiang Mai, Khon Kaen, Bangkok, Rayong, and Songkhla. *AOT* data, obtained from satellite images captured by the TERRA/AQUA satellite with the MODIS sensor system (MOD04 MYD04 products, with 109 images selected through the year of 2017, is also incorporated.

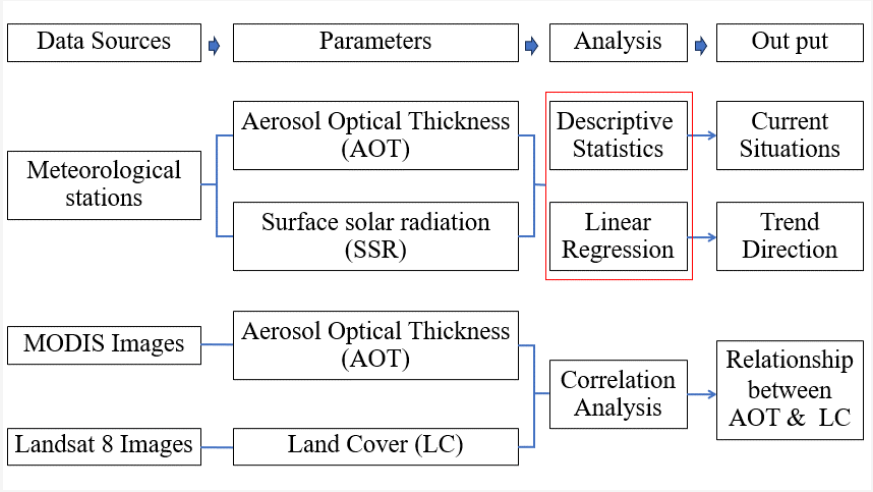

Figure 1: The study workflow

These images have a spatial resolution of 3 kilometers and were acquired from the LAADS DAAC agency (https://ladsweb.modaps.eosdis.nasa.gov/). The *AOT* values derived from satellite images are corrected by converting the Digital Number (DN) data to the corresponding *AOT* values using an established equation. The equation used to calculate Aerosol Optical Thickness (*AOT*) derived from MODIS is expressed as follow:

$$AOT = a \cdot DN + b$$

Equation 1

where:

AOT = Aerosol Optical Thickness
a = the scale factor (0.001)
DN = Digital Number
b = the offset (0.0)

To categorize the *AOT* values obtained for aerosols in the atmosphere, they were divided into seven ranges. The ranges were defined as follows: range 1 for values below 0, range 7 for values above 1, and ranges 2 to 6 with intervals of 0.2 for values in between. The land cover information for the five cities was derived from Landsat 8 satellite images captured in February 2017. All images underwent necessary corrections, including coordinate and radiometric corrections to ensure accurate and reliable data. Equation 2 was applied for radiometric correction, expressed as follow:

$$TOA\ planetary\ reflec\tan ce = \frac{M_\rho Q_{cal} + A_p}{\mathrm{Sin}(\theta_{se})}$$

Equation 2

where:

M_ρ = band-specific multiplicative rescaling factor obtained from the metadata REFLECTANCE_MULT_BAND_x, where 'x' denotes the band number)
A_ρ = band-specific additive rescaling factor from the metadata REFLECTANCE_ADD _BAND_x)
Q_{cal} = quantized and calibrated standard product pixel values (DN)

Subsequently, the obtained satellite images were investigated with an unsupervised classification method. With distinct spectral patterns, there could be 15-16 different types of land cover depending on the city. The ground survey was then conducted at thirty randomly chosen checkpoints for each land cover category to verify the land cover interpretation. Furthermore, sampling areas of land cover types were used for the supervised method so that the automatic classification of visual data with statistical grouping could make use of spectral patterns of different objects on the earth's surface. Sample areas of each land use type are received (training area) and this statistical value is then used to analyze the area in the entire image. Additionally, high-resolution satellite images (Pléiades) were used to perform visual image interpretation, allowing for further validation. Ultimately, the relationship between *AOT* and land cover ratio was analyzed with multiple regression. As land cover refers what covers the surface of the earth such as water, grassland, forest, bare soil etc. [30], the land cover in this study was categorized into nine types: aquaculture areas, water bodies, areas prepared for cultivation, paddy field, sparse forest, forests, built-up areas, open spaces, and orchard.

Multiple regression models with correlated independent variables have multicollinearity. This may negatively impact regression results. Thus, regression multicollinearity is measured by variance inflation factor (VIF), which can quantify how much a regression coefficient's variance is inflated due to multicollinearity.

3. The Study Areas

Thailand is located between latitudes 5 ° 37′ N and 20 ° 27′ N and between longitudes 97 ° 22′ E and 105 ° 37′ E, and its total area is approximately 513,115 square kilometers. Thailand was divided into five regions based on climate: the northern region, the northeastern region, the eastern region, the central region, and the southern region [31]. According to Koppen's classification system, the climate is classified as a tropical climate, in which there is an abundance of rainfall and year-round high temperatures. The average temperature of the coolest month is above 18 degrees Celsius. It can be divided further into three sub-climatic zones: (1) Tropical wet-dry climate or Tropical savannah climate (Aw) is the majority of climate in Thailand are the northern, northeastern, central, western, northern, and western of east regions. This region will experience rainy and arid seasons that alternate and are markedly distinct. In other words, there will be rain throughout the southwest monsoon season. In contrast, the northeast monsoon season or winter is arid. (2) Tropical monsoon climate (Am) is a climate characterized by abundant rainfall. However, there will be at least three months without more than 62 millimeters of precipitation. In west coast of southern region and eastern region of Thailand are characterized by this climate. (3) Tropical rainforest climate (Af) is a climate characterized by year-round precipitation. Typically, more than 1,500 millimetres of precipitation falls annually. There is in the east coast of southern region [32].

The study examines the occurrence of the global dimming phenomenon in Thailand, and with a specific focus on Bangkok, the capital city, as well as four chosen regional major cities: Chiang Mai in the northern region, Rayong in the eastern region, Khon Khen in the northeastern region, and Songkla in the southern region, for clarifying the relationship between land cover and *AOT*. The selection of these locations aims to inclusively encompass various geographical regions within Thailand, in order to facilitate an exhaustive investigation of the dimming phenomenon. The spatial distribution of the study areas is depicted in Figure 2.

4. Results and Discussions

4.1 The Current State of Aerosol Optical Thickness in Thailand

Aerosols are a complex mixture of solid and liquid particles that are suspended in the Earth's atmosphere. They comprise a wide range of substances, including sea salt particles, volcanic ash, smoke from wildfires, and pollutants emitted from manufacturing processes. These aerosols possess the ability to impact the Earth's climate by either contributing to the process of warming or cooling. Additionally, they have the capacity to influence the process of cloud formation, either facilitating or impeding it. Moreover, the inhalation of aerosols might result in detrimental impacts on human health. The influence of atmospheric aerosols on solar radiation is contingent upon their size and composition [33]. According to NASA [34], these objects possess the ability to either reflect or absorb solar radiation, both directly and indirectly. They may act as a catalyst for cloud or ice formation, thereby exerting a cooling effect that can counterbalance the warming effects of increased CO_2 concentrations.

The Aerosol Optical Thickness (*AOT*) is the degree to which aerosol prevent the transmission of light in the atmosphere [35]. Values of *AOT* below 0.1 are indicative of favorable atmospheric conditions characterized by clear sky and optimal visibility. Conversely, values reaching up to 4 denote the existence of significantly concentrated aerosols, which might provide difficulties in observing the sun even during daytime hours [33]. According to meteorologic stations provided in only a major city of each region, it is remarked that hereby results may not exactly explain for the variability within each region of Thailand; however, as it is data of major city; therefore, it could be indicated for a holistic picture for the region. The examination of *AOT* levels in different locations indicates that the central region of Thailand displays the highest average annual *AOT* of 0.619. This is followed by the Northeast, North, and South regions, which exhibit *AOT* values of 0.582, 0.579, and 0.481, respectively. When considering seasonal fluctuations, it is shown that the northern region shows the greatest average *AOT* values of 0.769 during summer and 0.633 during the rainy seasons. For the winter, the central region has the highest recorded average *AOT* of 0.552. Moreover, upon analysis of the mean monthly *AOT* values, it is evident that the northern region displays the highest average *AOT* of 0.921 in March.

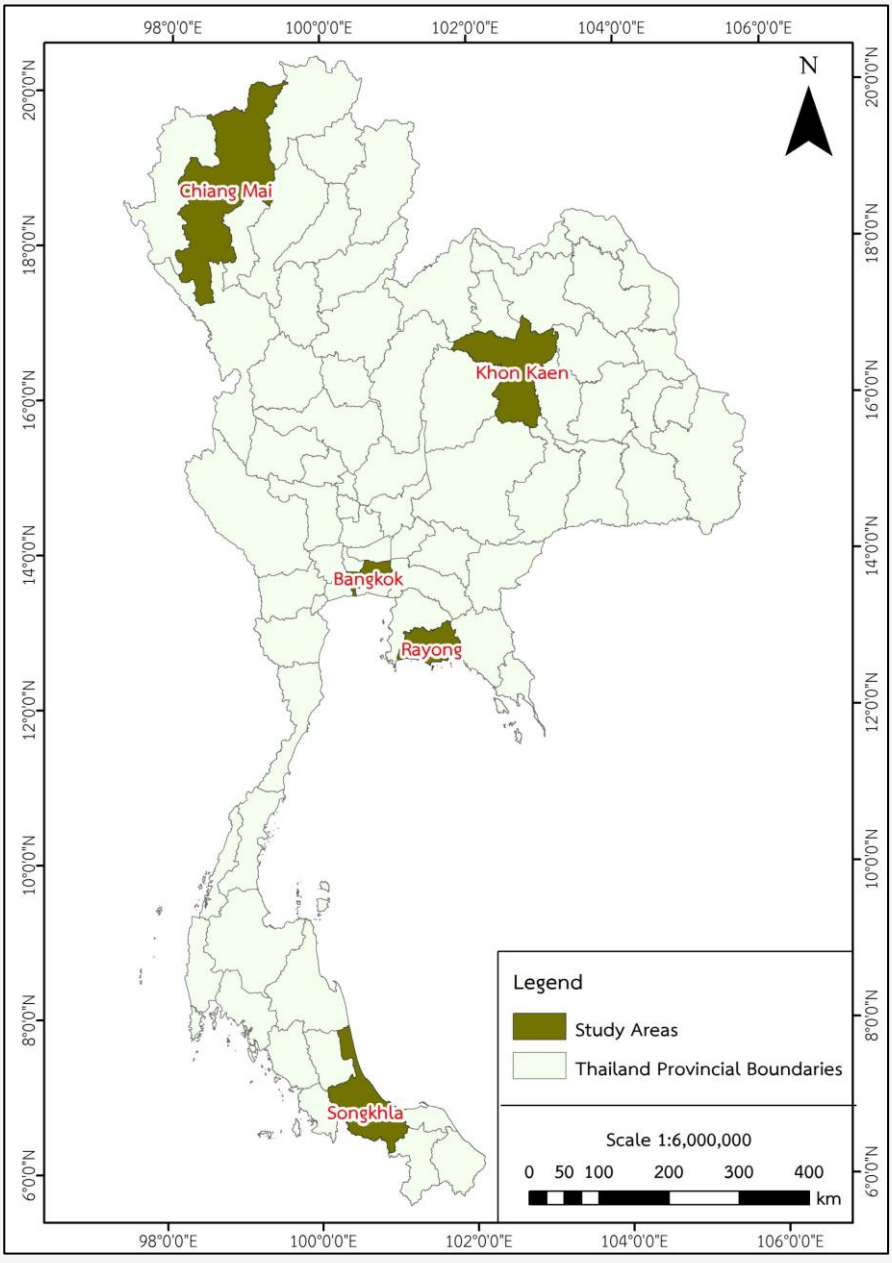

Figure 2: Study areas

Similarly, the northeastern and central regions also demonstrate notable *AOT* averages during this period, with values of 0.877 and 0.788, respectively (Table 1). The results, when compared to the defined criteria of clear skies with an *AOT* of below 0.1, suggest that the current atmosphere in Thailand contains aerosol particles that diminish the solar radiation reaching the Earth's surface. However, if the monthly *AOT* trend during 2003 – 2017 was taken into consideration, the Mann-Kendell test did not indicate any statistically significant of the trend.

4.2 The Variations in Surface Solar Radiation Intensity

Global dimming refers to the phenomenon characterized by a reduction in the intensity of solar radiation reaching the Earth's surface. The scientific scrutiny and examination of global dimming commenced during the 1950s, unveiling a discernible decline in the intensity of solar radiation from the 1950s to the 1980s. Nevertheless, a shift towards brightening, indicating an increase in solar radiation intensity, has been generally observed after 1990.

Table 1: *AOT* averages by region from 2003 to 2017

Region	*AOT* averages				The month with the highest average
	Yearly	Summer	Rainy	Winter	
North	0.579	0.769	0.633	0.349	March (0.921)
Northeast	0.582	0.690	0.555	0.458	March (0.877)
Central	0.619	0.672	0.604	0.552	March (0.788)
South	0.481	0.456	0.568	0.434	September (0.602)
Thailand	0.575	0.671	0.591	0.463	March (0.789)

Table 2: Estimate slope of the trend line for the regions' average annual and seasonal solar radiation intensity from 1951 to 1990

Region	Estimate slope of the trend line (Q_{med})			
	Annual	Summer	Rainy	Winter
Central	0.09142	0.08032	0.30782	0.13016
North	0.04122	-0.08250	0.11414	-0.05273
Northeast	-0.17900**	-0.19780*	-0.12585	-0.16776*
West	-0.28545*	-0.47347**	-0.17209	-0.21030
South	-0.19907**	-0.54503***	-0.09294	0.04840
Country	0.03395	-0.07503	0.05291	0.10666

Remark: *Statistically significant at the 0.05 level
**Statistically significant at the 0.01 level
***Statistically significant at the 0.001 level

Consequently, the period can be divided into two distinct phases: the dimming period before 1990 and the subsequent brightening period. The year 1990 is a significant milestone for examining alterations in surface solar radiation intensity occurrences within the geographical region of Thailand.

It is imperative to acknowledge that there are inherent constraints in gathering surface solar radiation measurements in Thailand. Due to the unavailability of direct data-gathering methods for examining the phenomenon prior to 1990, this research employed other procedures. The solar radiation intensity data was predicted by comparing variables rather than the direct measurement of solar radiation intensity. In this study, the researchers utilized a model developed by Chanchai [29] to predict the mean daily aggregate radiation for each month. In order to evaluate the trajectory of solar radiation intensity alterations on the Earth's surface in the post-1990 period (1995-2017), this study employed data from several sources, encompassing AERONET (1 station), NASA (1 station), the Meteorological Department (5 stations), the Pollution Control Department (57 stations), and the Department of Alternative Energy Development and Efficiency (39 stations).

4.2.1 The temporal pattern of solar radiation intensity fluctuations before to 1990

The estimating model used to calculate the mean daily total radiation was developed by an analysis of the disparity between the average daily maximum and minimum air temperatures, in addition to the coefficients integrated into the equation. The dataset included data collected from 19 air quality monitoring sites located in Thailand, covering the period from 1951 to 1990. The results indicate a persistent and increasing pattern in the mean annual solar radiation intensity in Thailand. The calculated slope of the trend was found to be 0.03395, as indicated in Table 2 and Figure 2. Regarding the seasonal aspect, it was observed that the trend slopes exhibited values of -0.07503 during the summer season, 0.05291 during the rainy season, and 0.10666 during the winter season. Furthermore, the mean values of solar radiation intensity for these seasons were determined as 230.03, 193.62, and 197.56 W/m^2, respectively. It is noteworthy to mention that the month of June had the most substantial decrease, as evidenced by a trend slope coefficient of -0.17288 and an average intensity of 206.45 W/m^2 (as depicted in Figure 3). Hence, it may be deduced that radiation in Thailand exhibited a statistically insignificant rising trend before 1990.

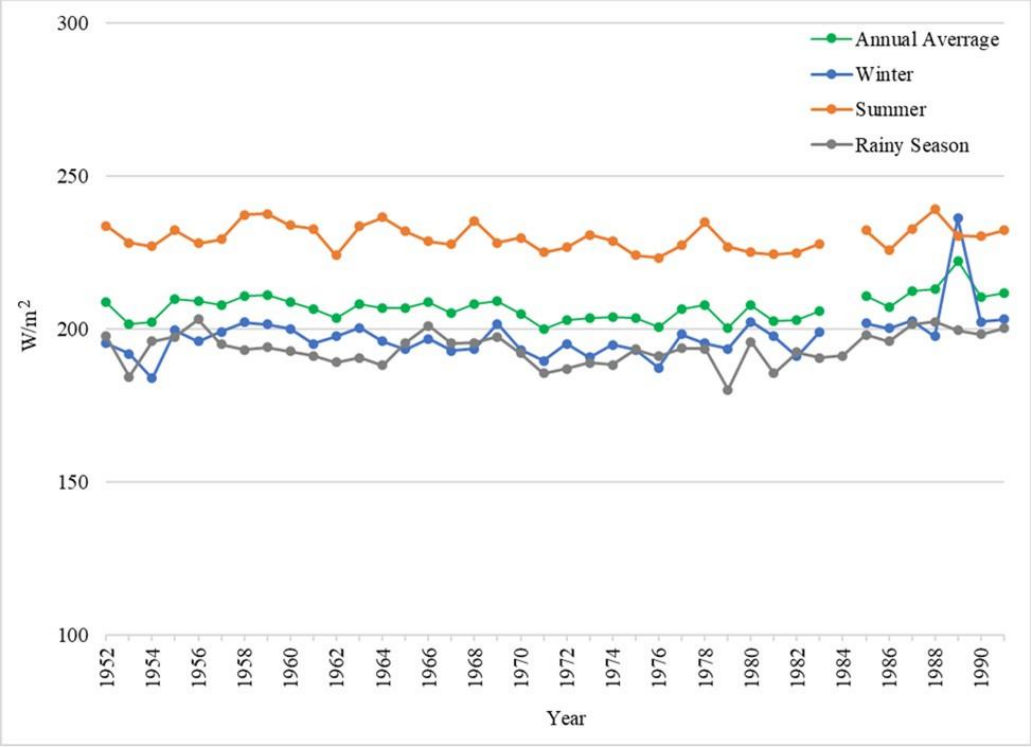

Figure 3: The annual and seasonal variations of solar radiation intensity from 1951-1990

The observed phenomenon can be attributed to the pre-1990 period in Thailand, which was during the process of initiating national development policies for improving the infrastructure in Bangkok and other major urban regions, involving the construction of various transportation networks, irrigation systems, electrical systems, and a wide range of energy infrastructures. However, the projects had not yet been fully implemented and the country enacted legislation on industrial investment, but with limited enforcement over the specified timeframe. Therefore, dust and pollutants resulting from human activities still have a low and insignificant role in reducing solar radiation, which might be attributed to the lack of the global dimming phenomenon observed during this period.

4.2.2 The temporal pattern of solar radiation intensity fluctuations after 1990

Analysis of solar radiation intensity after the year 1990 reveals a distinct shift in the surface solar radiation (*SSR*) situation. Unlike the period before 1990, where *SSR* intensity tended to increase statistically significantly, the post-1990 era experienced noteworthy variations.

To investigate the changes in solar radiation intensity during the years 1995 to 2017, data from 102 air quality monitoring stations across Thailand were employed. Among these stations, 90 had sufficient data for trend analysis. As shown in Figure 4 and Table 3, the average annual solar radiation intensity in Thailand exhibits a negligible decreasing trend, with a calculated slope of approximately -0.104, according to the findings of this study. Winter and summer exhibit a slight decrease in average solar radiation intensity, whereas the rainy season displays a slight increase. The calculated slope values for each season are -0.022 in summer, 0.052 in the rainy season, and -0.342 in winter, with mean values of 223.65 W/m^2, 195.23 W/m^2, and 194.77 W/m^2, respectively. Moreover, when examining regional data, it is observed that the annual average solar radiation intensity in the central and eastern regions exhibits a decreasing trend, whereas the intensity in other regions exhibits an increasing trend. Notably, the average solar radiation intensity in the western region is the highest of all regions studied. After 1990, the intensity of solar radiation decreased, suggesting that Thailand would initially encounter dimming.

Table 3: Estimate slope of the trend line for the regions' average annual and seasonal solar radiation intensity from 1995 to 2017

Region	Estimate slope of the trend line (Q_{med})			
	Annual	Summer	Rainy	Winter
Central	-0.510	-0.167	-0.560*	-0.900*
North	0.701	0.700	-0.099	1.272
Northeast	1.230*	1.381*	1.193**	0.716
East	-0.228	-0.311	0.413	-0.081
West	2.228***	2.070*	1.303*	2.268**
South	0.638	0.807	0.391	-0.369
Country	-0.104	-0.022	0.052	-0.342

Remark: *Statistically significant at the 0.05 level
**Statistically significant at the 0.01 level

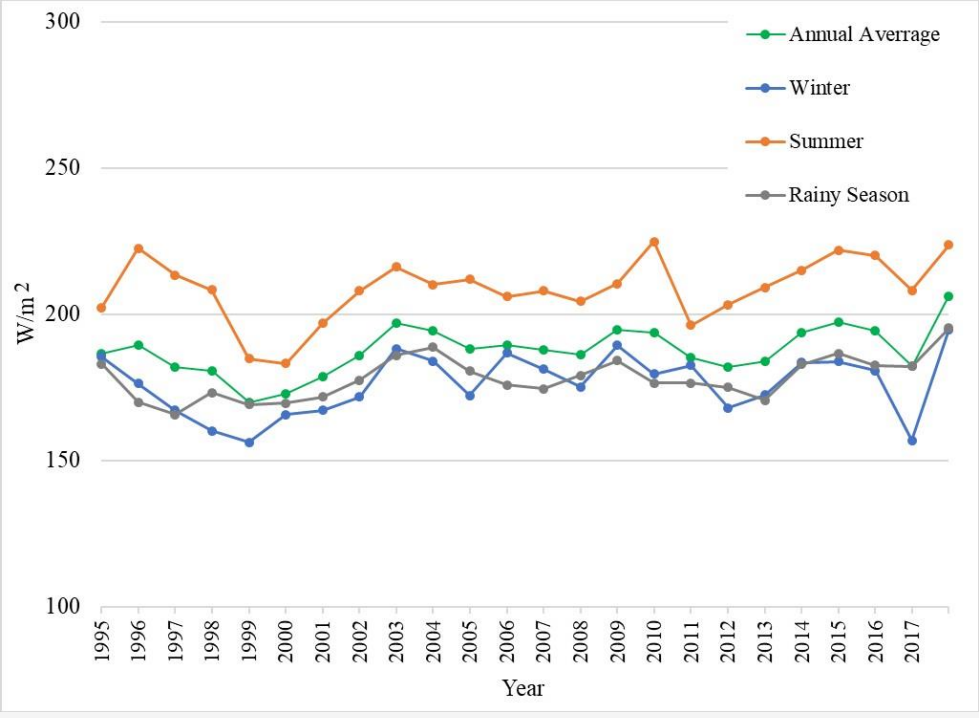

Figure 4: The annual and seasonal changes in solar radiation intensity of Thailand from 1995-2017

4.3 The correlation between the Aerosol Optical Thickness (AOT) and Land Cover Ratio

4.3.1 The spatial distribution of AOT

The spatial distribution of *AOT* in Thailand varies considerably between distinct regions (Figure 5). In 2017, the *AOT* levels are consistently higher in the country's central region, particularly during the months of February, March, and April. This trend is also observed in the northern and northeastern regions, where *AOT* concentrations increase significantly during the months of March and April. In contrast, the southern region generally shows lower *AOT* levels, attributed in part to specific climatic factors such as wind direction and rainfall. However, it is important to note that limited data is available for the southern region, which may affect the comprehensiveness of the analysis. The rainy season presents challenges for satellite imaging due to frequent cloud cover, resulting in some areas lacking sufficient information to analyze the optical thickness of aerosols effectively. Overall, the study highlights the spatial heterogeneity of aerosol distribution characteristics across Thailand, indicating the need for further research and data collection to better understand the factors influencing aerosol variations in different regions and seasons.

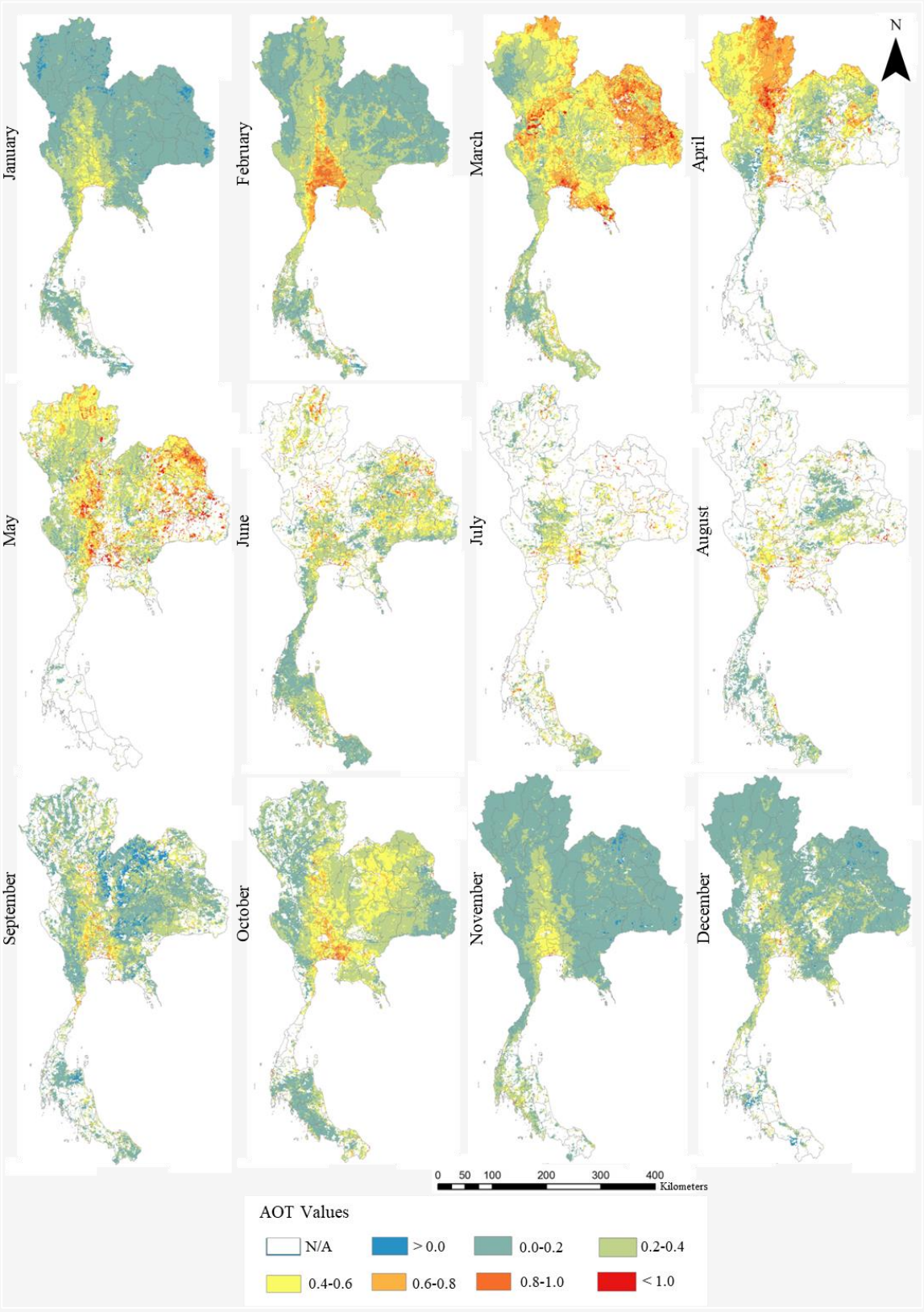

Figure 5: Distribution of monthly *AOT* throughout Thailand in 2017

4.3.2 Land Cover in Thailand

Table 4 shows the proportions of land cover for five provinces — Bangkok, Rayong, Chiang Mai, Khon Kaen, and Songkhla — and distinct land use properties were observed. Bangkok, the capital of Thailand and economic center, has a distinctive landscape, with the highest proportion of buildings (58.33%), followed by agricultural areas (34.05%), sparse forests (5.10%), water bodies (2.19%), and open spaces (0.3%). The majority of land cover in Rayong Province is agricultural land (63.63%), followed by buildings (18.46%), forests (10.74%), sparse forests (3.61%), water bodies (3.32%), and open spaces (0.25%). In Chiang Mai, forests comprise 56.7% of the total land area, followed by sparse forests (28.41%), agricultural land (6.76%), open spaces (4.65%), buildings (2.99%), and bodies waters (0.51%). Khon Kaen has the maximum proportion of agricultural land at 43.24 %, followed by forests (22.71 %), buildings (22.08 %), open spaces (10.01 %), and areas of water (1.7 %). Agriculture comprises 28.92% of the land area in Songkhla Province, followed by water bodies at 18.75%, open spaces at 13.90%, forests at 13.566%, buildings at 12.48%, and sparse forests at 12.33%. The western regions of Songkhla province are occupied by agricultural land and are abundant water sources due to the presence of a lake. Forested areas surround the province.

Land use patterns and resource allocation in each Thai province are influenced by a variety of factors, including topography, economic activities, and urbanization. These factors play a significant role in determining the distribution of land cover and the overall environmental and climatic conditions of each region. Bangkok's physical characteristics as a central plain have fostered intense urbanization and economic development, resulting in a preponderance of buildings and densely populated areas, whereas agricultural lands encompass the city. The mostly flat terrain of Rayong has resulted in extensive agriculture, while areas near the coast have seen a greater concentration of residential and industrial estates. In Chiang Mai, for example, the mountainous terrain contributes to the dense and sparse forest cover, whereas the basin plains contain the majority of usable areas, such as buildings, agricultural land, and vacant land. Similarly, the plateau topography in Khon Kaen influences the predominance of agricultural land use, with forest and water concentrated in the province's northern region. In Songkhla, the prevalence of water bodies such as Songkhla Lake has made it an indispensable source of water for the surrounding agricultural areas. Forests are dispersed throughout the province, contributing to the overall distribution of land cover (Figure 6).

The land cover distribution data provides valuable insights into Thailand's variegated landscape across its various regions. In addition, it emphasizes the impact of urban activities on the environment and climate, as urbanization has been linked with changes in land use, air quality, and heat island effects. Understanding these relationships is essential for sustainable development and effective environmental management in each province and across the country.

Table 4: The Proportion of land use/cover in Bangkok, Rayong, Chiang Mai, Khon Kaen, and Songkla

Province		Land Use/Cover						Total
		Forest	Sparse forest	Water body	Agriculture	Open space	Built-up area	
Bangkok	Area (km^2)	-	80.19	34.38	535.06	5.10	916.51	1,571.23
	%	-	5.10	2.19	34.05	0.33	58.33	100.00
Rayong	Area (km^2)	398.83	134.01	123.47	2,363.93	8.71	685.72	3,714.68
	%	10.74	3.61	3.32	63.63	0.24	18.46	100.00
Chiang Mai	Area (km^2)	12,513.71	6,269.45	111.84	1,491.43	1,025.13	658.70	22,070.25
	%	56.70	28.41	0.51	6.76	4.65	2.99	100.00
Khon Khen	Area (km^2)	2,563.88	27.82	194.06	4,881.98	1,129.82	2492.60	11,290.17
	%	22.71	0.25	1.72	43.24	10.01	22.08	100.00
Songkla	Area (km^2)	1,065.8	974.07	1,473.542	2,272.8	1,092.518	980.627	7,859.357
	%	13.56	12.39	18.75	28.92	13.90	12.48	100.00

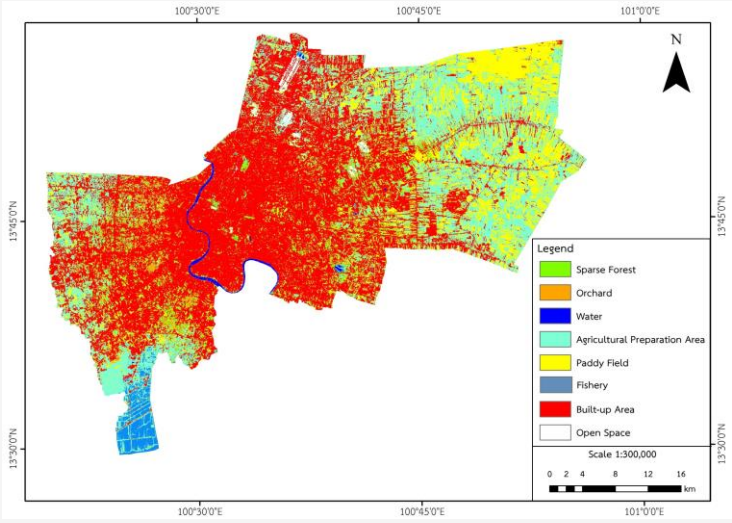

Bangkok

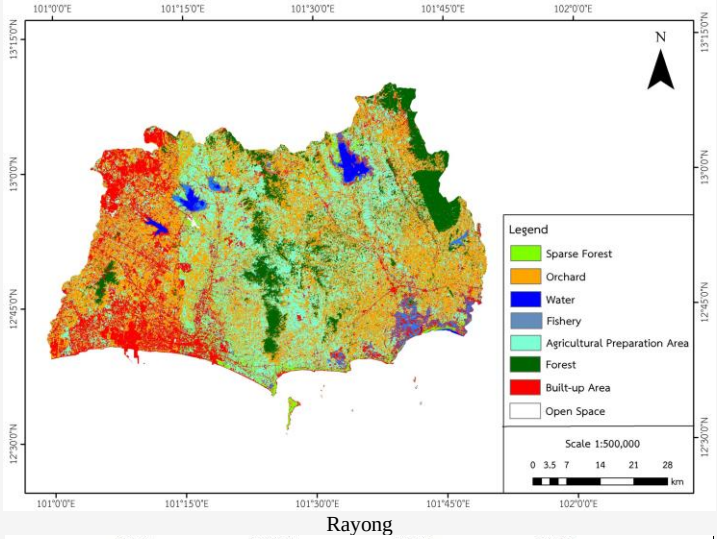

Rayong

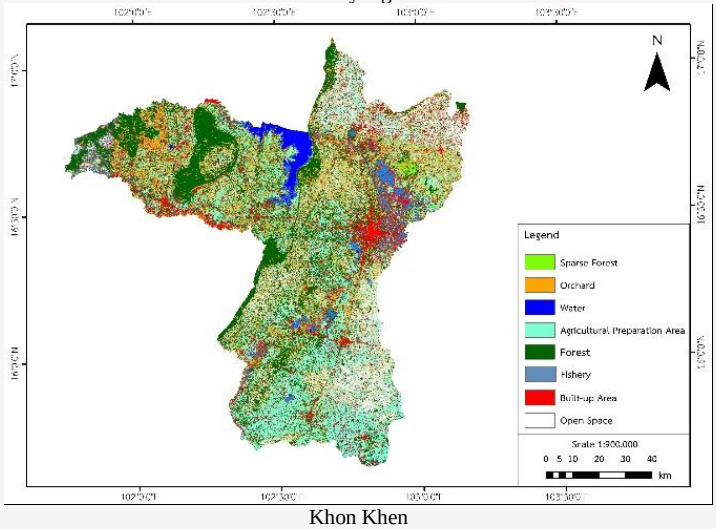

Khon Khen

Figure 6: Land Use/Cover in Thailand's five provinces (continue next page)

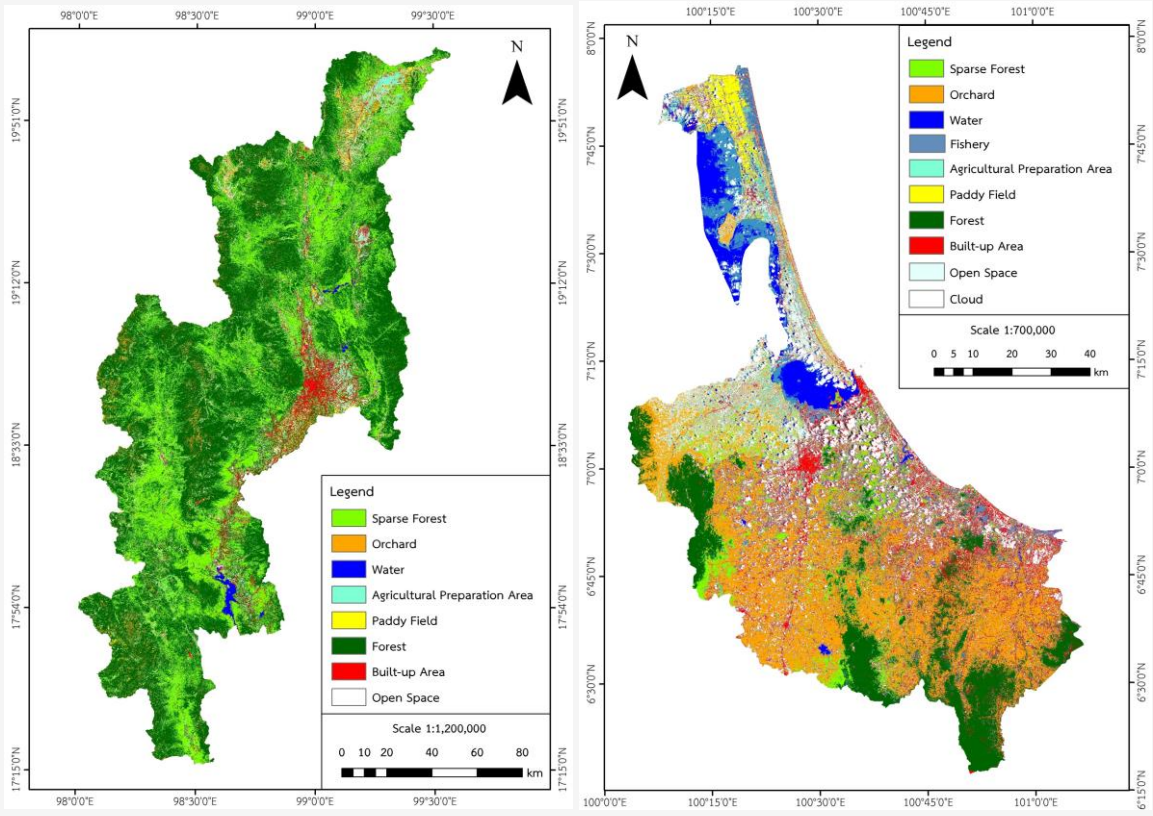

Figure 6: Land Use/Cover in Thailand's five provinces (continue from previous page)

4.3.3 The correlation between AOT and land use/cover

This section tries to produce empirical evidence of the link between land cover and aerosols by rigorous statistical analysis, allowing a better understanding of the processes controlling aerosol distribution and behavior in different locations. The findings will help to advance our understanding of aerosol-related climate dynamics and aid in the development of effective solutions to solve aerosol-related concerns for environmental conservation and climate change mitigation.

It is critical in multiple regression analysis to guarantee that each independent variable remains independent of the others [36]. We use Tolerance and Variance Inflation Factor (VIF) statistics to determine the degree of dependency among independent variables. A close to zero tolerance value or a high VIF value implies a strong link between the independent variable and other factors. The independent variable in this study is the proportion of land cover derived from Landsat 8 imagery in 2017, which was divided into five kinds in order to examine its independence. "Built-up area" was chosen as the dependent variable for the test regression equation. Table 5 displays the Tolerance and VIF values determined by statistical analysis for each land cover group. According to the results, all variables have values larger than 0.5, indicating an appropriate level of independence. Consequently, these land cover variables were employed as independent variables to construct a link between atmospheric aerosol optical thickness and land cover proportions.

A statistical tool was used in this work to generate a linear regression equation to establish the relationship between the optical thickness of atmospheric particles and the proportion of land cover. The Stepwise technique was used to identify the independent variables that are most closely related to the dependent variable (*AOT*). The regression equation is presented in Table 6, Based on the significance level of the test statistic F, 0.05, two independent variables, "build-up area" and "forest," satisfied the criteria and were included in the regression equation. Equation 2 (b), the chosen regression equation, produced the highest coefficient of determination (R), with an R-value of 0.841. This suggests that there is a strong relationship between *AOT* and land cover.

Table 5: Tolerance and VIF values of Land Use/Cover

Model	Collinearity Statistics	
	Tolerance	VIF
Sparse forest	0.481	2.078
Forest	0.472	2.120
Agriculture	0.462	2.163
Water body	0.629	1.591
Open space	0.451	2.217

a. Dependent Variable: Built-up area

Table 6: The regression equation between *AOT* and land cover ratio

Model	R	R^2	Adjusted R^2	Std. Error of the Estimate	Change Statistics					Durbin-Watson
					R^2 Change	F Change	df1	df^2	Sig. F Change	
1	0.776[a]	0.602	0.596	0.08092	0.602	95.403	1	63	0.000	
2	0.841[b]	0.708	0.698	0.06995	0.105	22.313	1	62	0.000	1.561

a. Predictors: (Constant), Built-up area
b. Predictors: (Constant), Built-up area, Forest
c. Dependent Variable: *AOT*

Table 7: F-values test between *AOT* and Land Use/Cover

Model		Sum of Squares	df	Mean Square	F	Sig.
1	Regression	0.625	1	0.625	95.403	0.000[b]
	Residual	0.413	63	0.007		
	Total	1.037	64			
2	Regression	0.734	2	0.367	74.996	0.000[c]
	Residual	0.303	62	0.005		
	Total	1.037	64			

a. Dependent Variable: *AOT*
b. Predictors: (Constant), Built-up area
c. Predictors: (Constant), Built-up area, Forest

Furthermore, the R^2 value of 0.708 indicates that variations in the proportion of the identified independent variables can explain 70.8% of the variation in *AOT*. The regression equation's standard error for estimating *AOT* was determined to be 0.069 units. Furthermore, the Durbin Watson value of 1.561 demonstrated that the equation's independent variables are independent of one another. We may better understand how different land cover factors contribute to changes in *AOT* by using this linear regression equation, which provides useful insights into the link between land use patterns and atmospheric aerosols. Table 7 provides the F test results for each equation. In the second regression equation, the significant value is 0.000, which is less than the predetermined significance level of 0.05. Therefore, it can be inferred that at least one independent variable is significantly associated with the aerosol optical thickness. To further ascertain the specific independent variables that are related to atmospheric aerosol optical thickness, we consider the coefficients presented in Table 8.

This table comprises constant values and regression coefficients of each variable representing the land cover ratio. The resulting regression equation with its components is as follow:

$$AOT = 0.254 + 0.002B - 0.003F$$

Equation 3

Where:
AOT = aerosol optical thickness
B = built-up area
F = forest coverage

It should be remarked that the resulting regression equation may vary by different proportion of land cover of the chosen regional major cities, as the land cover data derived from a capital city of the region while *AOT* can vary significantly from one location to another. In the regression equation, the standard error of the constant (intercept) is 0.026, demonstrating the precision of calculating the baseline value.

The standard error of the coefficient for "Building area" is 0.000, while it is 0.001 for "Forest area." These standard errors reflect the variability of the data and represent the accuracy of the estimated coefficients. The Beta values represent the relationship between the independent factors and *AOT*. The "Building area" has the highest Beta value of 0.511 in this scenario, suggesting the strongest positive association with *AOT*. On the other hand, the "Forest area" has a Beta value of -0.419, indicating a negative association with *AOT*.

The t-test significant values for the proportion of land cover types, specifically "Building area" and "Forest area," are both 0.000, which is less than the 0.05 significance level. This result shows that the "Building area" and "Forest area" are statistically significant and considerably impact *AOT*. These findings are consistent with the F-test statistic values in Table 7. The low p-values confirm the importance of these factors in the regression equation and their influence on *AOT*. To investigate the linear regression analysis circumstances (Equation 1), we must examine the following assumptions.

The mean error in the regression equation is determined to be zero, showing that the errors are balanced around zero on average (Table 9). The error must have a normal distribution: Figure 7 depicts the error distribution, which appears to be about normal. However, a tiny pattern in the residual scatterplot may indicate some deviations from perfect normality. Tolerance must be independent. This requirement is satisfied by the Durbin-Watson test value of 1.561, which demonstrates that the tolerance is independent. The error variance must be constant for all X values. As illustrated in Figure 7, the error distribution has a non-constant variance, implying that the assumption of homoscedasticity may not apply.

Based on these conditions, the regression equation (Equation 1) is thought to be somewhat dependable. The proportion of land cover influences approximately 70.8% of the fluctuations in *AOT*, whereas other factors impact the remaining 29.2%. The coefficients of the independent variables show that increasing the proportion of building area leads to an increase in aerosol optical thickness, whereas raising the proportion of forest area results in a decrease in aerosol optical thickness. It is possible to conclude that human-induced aerosols, particularly in locations with massive construction densities, have an important role in affecting *AOT*, hence influencing solar radiation intensity at the Earth's surface.

Table 9: The error in the regression equation between *AOT* and land cover ratio

	Minimum	Maximum	Mean	Std. Deviation	N
Predicted Value	0.1410	0.4221	0.2793	0.1088	65
Residual	-0.14387	0.18828	0.00000	0.06596	65
Std. Predicted Value	-1.270	1.311	0.000	1.000	65
Std. Residual	-2.129	2.787	0.000	0.976	65

a. Dependent Variable: *AOT*

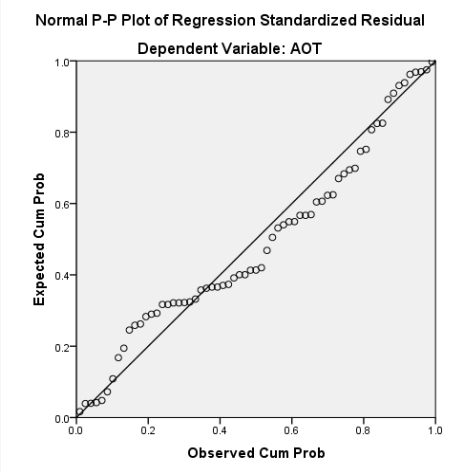

(a)

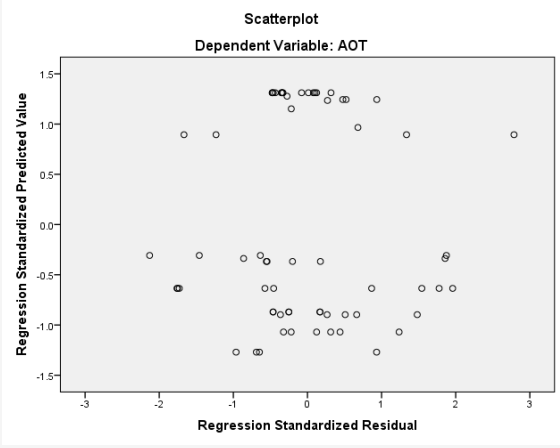

(b)

Figure 7: (a) The normal distribution of errors in the regression (b) Distribution characteristics of the variance of the tolerance between *AOT* and land cover ratio

5. Conclusion

Aerosols in the atmosphere have an important part in affecting the global dimming phenomenon. Aerosols have special characteristics that can either scatter solar radiation back into space or absorb solar radiation within the atmosphere, preventing it from reaching the Earth's surface. Aerosols' specific radiative effects are determined by their composition, which consists of sulfate, soot (black carbon), and particle matter. Aerosols, for instance, can reflect up to 50% of incoming solar radiation [3], or more than 5 times the solar radiation in some cases [37]. These aerosol concentrations are especially noticeable in highly populated areas, where anthropogenic activities such as automotive emissions contribute significantly to aerosol formation [4]. The increased number of automobiles and industrial operations in these locations increases aerosol emissions into the atmosphere, further affecting the radiation balance and climate.

Prior to the 1990s, the phenomena of a change from dimming to brightening was observed in areas with a lot of industry and transportation. After the 1990s, however, production facilities shifted to underdeveloped countries, while wealthier nations embraced cleaner technologies, which decreased the phenomenon of dimming and resulted in the development of brightening patterns. The actual evidence for the dimming phenomenon in Asia and Africa, particularly in Thailand, is still lacking. Therefore, the purpose of this research is to look at Surface Solar Radiation (SSR) and Aerosol Optical Thickness (*AOT*) patterns before and after the 1990s and correlations of *AOT* and land use in five provinces: Bangkok, Chiang Mai, Songkla, Rayong, and Kon Khen.

The study revealed notable patterns in the average annual solar radiation intensity trend in Thailand. Prior to 1990, the analysis, based on the estimation model of average daily radiation and temperature range during the day, indicated changes in solar radiation intensity tend to increase. Northeast and east regions have statistically significant increases in every season. However, during the latter period of 1990 onwards, a substantial decrease in annual average solar radiation intensity was observed, particularly in the central and eastern regions. Notably, the summer and winter seasons exhibited a decreasing shift in solar radiation intensity in central and eastern regions.

The study found that the Aerosol Optical Thickness (*AOT*) trend has not increased significantly. However, in each season, it is found that *AOT* in the summer season of the central region tends to increase at a significant level of 0.05. Regarding changes in monthly, the highest *AOT* in Thailand was found in March, with a value of 0.789. According to the average annual solar radiation intensity (SSR_{avg}) trend in Thailand, it has not significantly changed during the year before 1990. In contrast, the SSR_{avg} of the country after 1990 showed a significant decrease with a significant level of 0.01 in the central, northern, and eastern regions. The tendency of solar radiation intensity has highly changed in the winter. The linear regression results showed that *AOT* is positively related to surface temperature. At the same time, a negative relationship was found with surface solar radiation intensity and relative humidity, with R^2 values equal to 0.285, 0.749, and 0.721, respectively. Moreover, *AOT* showed a positive relationship with building cover types while negative with forest cover types, with R^2 equal to 0.708. As per previous results, it was indicated that Thailand has been entering into a period of global dimming. Another result found that the influences of vegetation index and urban cover types have changed *AOT* situation. Therefore, it could alleviate air pollution by managing land covers in three characteristics: urban, agricultural, and forest. The management of plant characteristics in each area can create a response and effectively alleviation in the future.

Additionally, the result of the multiple regression equation between *AOT* and land covers showed that there is a positive relationship with buildings in positive and forests in negative with R^2 equal to 0.708, which means 70.8 percent of the *AOT* value changes caused by the influence of the change in the type of land cover "Buildings" and / or "forests" by increasing the building area in every 1% while the forest area remains the same. This increases *AOT* value by 0.002; on the contrary, if the building area has not been changed, but the forest area increases every 1%. The result will give the *AOT* value decreased by 0.003 and if the building area increases by 1% and the forest area declines 1% will result in *AOT* increasing by 0.005 units, which is consistent with the *AOT* inversely correlated to the vegetation index (*NDVI*). These findings will aid in identifying potential solutions to global dimming in Thailand while addressing the bigger issue of global warming. As a result, it is critical for Thai society to obtain a thorough grasp of the effects of global dimming.

Acknowledgements

The Biodiversity-based Economy Development Office (BEDO), Thailand, provided funding for the research. The dataset was contributed by the Hydro-Informatics Institute (Public Organization), the Department of Alternative Energy Development and Efficiency, the Department of Pollution Control, and the Thailand Meteorology Department.

References

[1] Stanhill, G. and Moreshet, S., (1992). Global Radiation Climate Change: the World Radiation Network. *Climatic. Change.*, Vol. 21, 57-75. https://doi.org/10.1007/BF00143253.

[2] Wild, M., (2009). How Well do IPCC-AR4/CMIP3 Climate Models Simulate Global Ddimming/Brightening and Twentieth-Century Daytime and Nighttime Warming?. *J. Geophys. Res*., Vol. 114(D00D11). https://doi.org/10.1029/2008JD011372.

[3] Ohmura, A., (2009). Observed Decadal Variations in Surface Solar Radiation and their Causes. *Journal of Geophysical Research*, Vol. 114(D10). https://doi.org/10.1029/2008JD011290.

[4] Alpert, A., Kishcha, P., Yoram, J. and Schwarzbard, R., (2005). Global Dimming or Local Dimming?: Effect of Urbanization on Sunlight Availability". *Geophysical Research Letters*, Vol. 32. https://doi.org/10.1029/2005GL023320.

[5] Alpert, P. and Kishcha, P., (2008). Quantification of the Effect of Urbanization on Solar Dimming. *Geophysical Research Letters*, Vol. 35, 1-5. https://doi.org/10.1029/2007GL033012.

[6] Stanhill, G., (1998). Long-term Trends in, and Spatial Variation of, Solar Irradiances in Ireland. *Int. J. Climatol*., Vol. 18, 1015–1030. https://doi.org/10.1002/(SICI)1097-0088(199807)18:9<1015::AID-JOC297>3.0.CO;2-2.

[7] Russak, V., (1990). Trends of Solar Radiation, Cloudiness and Atmospheric Transparency during Recent Decades in Estonia. *Tellus Ser. B*, Vol. 42, 206–210. https://doi.org/10.1034/j.1600-0889.1990.t01-1-00006.x.

[8] Liepert, B. G., Fabian, P. and Grassl, H., (1994). Solar Radiation in Germany: Observed Trends and Assessment of their Causes: Part I. Regional Approach. *Contrib. Atmos. Phys*., Vol. 67, 15– 29.

[9] Ohmura, A. and Lang, H., (1989). Secular Variation of Global Radiation in Europe. *IRS'88: Current Problems in Atmospheric Radiation,* J. Lenoble and J. F. Geleyn, Ed. Hampton, VA: A. Deepak Publ., 1989, 298–301.

[10] Aksoy, B., (1997). Variations and Trends in Global Solar Radiation for Turkey. *Theor. Appl. Climatol*., Vol. 58, 71–77. https://doi.org/10.1007/BF00867433.

[11] Stanhill, G. and Ianetz, A., (1997). Long-term Trends in, and the Spatial Variation of, Global Irradiance in Israel. *Tellus Ser. B*., Vol. 49, 112–122. https://doi.org/10.3402/tellusb.v49i1.15954.

[12] Abakumova, G. M., Feigelson, E. M., Russak, V. and Stadnik, V. V., (1996). Evaluation of Long-term Changes in Radiation, Cloudiness and Surface Temperature on the Territory of the Former Soviet Union. *J. Clim*., Vol. 9, 1319 – 1327. https://doi.org/10.1175/1520-0442(1996)009<1319:EOLTCI>2.0. CO;2.

[13] Norris, J. R. and Wild, M., (2007). Trends in Aerosol Radiative Effects over Europe Inferred from Observed Cloud Cover, Solar "Dimming," and Solar "Brightening", *J. Geophys. Res*., Vol. 112(D08214). https://doi.org/10.1029/2006JD007794.

[14] Stanhill, G. and Kalma, J. D., (1995). Solar Dimming and Urban Heating at Hong Kong. *Int. J. Climatol*., Vol. 15, 933– 941. https://doi.org/10.1002/joc.3370150807.

[15] Shi, G. Y., Hayasaka, T., Ohmura, A., Chen, Z. H., Wang, B., Zhao, J. Q., Che, H. Z. and Xu L., (2008). Data Quality Assessment and the Long-term Trend of Ground Solar Radiation in China. *J. Appl. Meteorol. Climatol*., Vol. 47, 1006–1016. https://doi.org/10.1175/2007JAMC1493.1.

[16] Ramanathan, V., Chung, C., Kim, D., Bettge, T., Buja, L., Kiehl, J. T., Washington, W. M., Fu, Q., Sikka, D. R. and Wild M., (2005). Atmospheric Brown Clouds: Impacts on South Asian Climate and Hydrological Cycle. *Proc. Natl. Acad. Sci. U. S. A*., Vol. 102, 5326 – 5333. https://doi.org/10.1073/pnas.0500656102.

[17] Norris, J. R. and Wild, M., (2009). Trends in Aerosol Radiative Effects over China and Japan Inferred from Observed Cloud Cover, Solar "Dimming," and Solar "Brightening,". *J. Geophys. Res*., Vol. 114, 1-11. https://doi.org/10.1029/2008JD011378.

[18] Omran, M. A., (2000). Analysis of Solar Radiation over Egypt. *Theor. Appl. Climatol*., Vol. 67, 225– 240. https://doi.org/10.1007/s007040070011.

[19] Power, H. C. and Mills, D. M., (2005). Solar Radiation Climate Change over South Africa and Assessment of the Radiative Impact of Volcanic Eruptions. *Int. J. Climatol*., Vol. 25, 295–318. https://doi.org/10.1002/joc.1134.

[20] Liley, B., (2009). New Zealand Dimming and Brightening. *J. Geophys. Res*., Vol. 114(D10). https://doi.org/10.1029/2008JD011401.

[21] Liepert, B. G., (2002). Observed Reductions of Surface Solar Radiation at Sites in the United States and Worldwide from 1961 to 1990. *Geophys. Res. Lett*., Vol. 29(10). https://doi.org/10.1029/2002GL014910.

[22] Cutforth, H. W. and Judiesch, D., (2007). Long-term Changes to Incoming Solar Energy on the Canadian Prairie. *Agric. For. Meteorol*., Vol. 145, 167–175. https://doi.org/10.1016/j.agrformet.2007.04.011.

[23] Stanhill, G. and Cohen, S., (1997). Recent Changes in Solar Irradiance in Antarctica. *J. Clim*., Vol. 10, 2078 - 2086. https://doi.org/10.1175/1520-0442(1997)010<2078:RCISII>2.0.CO;2.

[24] Stanhill, G., (1995). Global Irradiance, Air Pollution and Temperature Changes in the Arctic. *Philos. Trans. R. Soc. A*, Vol. 352, 247–258. https://doi.org/10.1098/rsta.1995.0068.

[25] Wild, M., (2008). Decadal Changes in Surface Radiative Fluxes and their Role in Global Climate Change. *Climate Variability and Extremes During the Past 100 Years (Advances in Global Change Research).* Vol. 33, S. Brönnimann, J. Luterbacher, T. Ewen, H.F. Diaz, R.S. Stolarski, U. Neu, Ed. New York: Springer, 2008, 155– 167.

[26] Sanchez-Lorenzo, A., Brunetti, M., Calbo, J. and Martin-Vide, J., (2007). Recent Spatial and Temporal Variability and Trends of Sunshine Duration over the Iberian Peninsula from a Homogenized Data Set. *J. Geophys. Res*., Vol. 112. https://doi.org/10.1029/2007JD008677.

[27] Kumari, B. P., Londhe, A. L., Daniel, S. and Jadhav, D. B., (2007). Observational Evidence of Solar Dimming: Offsetting Surface Warming over India. *Geophys. Res. Lett*., Vol. 34. https://doi:10.1029/2007GL031133.

[28] Riihimaki, L. D., Vignola, F. E. and Long, C. N., (2009). Analyzing the Contribution of Aerosols to an Observed Increase in Direct Normal Irradiance in Oregon. *J. Geophys. Res*., Vol. 114. https://doi:10.1029/2008JD010970.

[29] Chanchai, S., (2014). *Solar Radiation*. Faculty of Science, Silpakorn University. Bangkok: Phethkasem pub.

[30] Horning, N., (2004). *Land Cover Classification Methods*. Version 1.0. American Museum of Natural History, Center for Biodiversity and Conservation. https://www.amnh.org/content/download/74344/1391366/file/land-coverclassification-methods.pdf

[31] The Meteorological Department. (2023). *Climate of Thailand.* (in Thai). [Online]. Available: https://www.tmd.go.th/info/ภูมิอากาศของประเทศไทย. [Accessed October 19, 2023].

[32] Chomchan, S., (2023). *Drought in Thailand*. Land Development Department. (in Thai). [Online]. Available: https://www.ldd.go.th/web_UNCCD/dryland/page1.htm. [Accessed October 19, 2023].

[33] The Earth Observatory., (n.d). *Aerosol Optical Depth*. [Online]. Available: https://earthobservatory.nasa.gov/global-maps/MODAL2_M_AER_OD. [Accessed Dec. 19, 2018].

[34] National Aeronautics and Space Administration (NASA)., (n.d). *Aerosol Optical Thickness.* [Online]. Available: https://neo.gsfc.nasa.gov/view.php?datasetId=MYDAL2_M_AER_OD. [Accessed Dec. 19, 2018].

[35] National Aeronautics and Space Administration (NASA), (2007). *Aerosol Optical Thickness*. [Online]. Available: http://web.archive.org/web/20071126083354/http://daac.gsfc.nasa.gov/PIP/shtml/aerosol_optical_thickness_or_depth.shtml. [Accessed Dec. 19, 2018].

[36] Vanichbancha, K. (2003). *The Application of SPSS for Windows to Analyze Data*. 6th edition. Bangkok: Dhammasarn Co., Ltd.

[37] Ruckstuhl, C., Philpona., R., Behrens, K., Collaud, M.C., Durr, B., Helmo, A., Matzler, C., Nyeki, S., Ohmura, A., Vuilleumier, L., Weller, M., Wehrli, C. and Zelenka, A., (2008). Aerosol and Cloud Effects on Solar Brightening and the Recent Rapid Warming. *Geophysical Research Letters,* Vol. 35. https://doi.org/10.1029/2008GL034228.